Development of MgB2-based, bulk supermagnets

Michael Rudolf Koblischka, Alex Wiederhold, Muralidhar Miryala, Kazuo Inoue, Thomas Hauet, Bruno Douine, Kévin Berger, Masato Murakami, Uwe Hartmann

Development of MgB_2-based bulk supermagnets

M. R. Koblischka, A. Wiederhold, M. Muralidhar, K. Inoue, T. Hauet, B. Douine, K. Berger, M. Murakami and U. Hartmann

***Abstract*—A series of disk-shaped, bulk MgB_2 superconductors (sample diameter 20 mm, reaction temperatures ranging between 750 °C and 950 °C) was prepared in order to improve the performance for superconducting supermagnets. These samples were characterized by magnetic and electric measurements in fields up to 7 T and at various temperatures 10 K < T < 35 K. The irreversibility lines, the current densities, the resistance and the achievable trapped fields were determined. To analyze the data, a scaling of the flux pinning forces, $F_p = j_c \times B$, was performed. The different scaling behavior of the samples prepared at low and high reaction temperatures is discussed considering the achieved microstructures.**

***Index Terms*—MgB_2, supermagnets, trapped fields, flux pinning forces.**

I. Introduction

SUPERCONDUCTING MgB_2 trapped-field magnets ("supermagnets") may find a large variety of commercial and industrial applications at temperatures around 20 K, especially in the medical field, e.g., for MRI instruments similar to the 123-cuprate high-T_c superconductors operating at liquid nitrogen temperature (77 K) [1,2]. The main reason for this is the character of the grain boundaries in MgB_2, which do not show a weak-link behavior like in the case of the cuprates [3-10]. The fabrication of bulk MgB_2 superconducting materials is even more attractive due to low fabrication cost and simpler processing since this material does not require a strong texture to reach a high enough critical current density, and eventually, high trapped field values around 20 K. Further, the smaller weight and a higher mechanical strength are other important factors for possible applications. On the other hand, problems arise due to percolative current flow in the polycrystalline samples, and due to the porous character of the bulk samples. Therefore, we prepared a series of samples with a diameter of 20 mm at various reaction temperatures in order to determine the optimum preparation conditions for bulk MgB_2 samples.

Manuscript received 07.03.2014.

M. R. Koblischka, A. Wiederhold and U. Hartmann are with the Institute of Experimental Physics, Saarland University, P.O.Box 151150, D-66041 Saarbrücken, Germany (phone: +49-681-302-4555; fax: +49-681-302-3790; e-mail: m.koblischka@mx.uni-saarland.de).

M. Muralidhar, K. Inoue and M. Murakami are with Superconducting Materials Laboratory, Department of Materials Science and Engineering, Shibaura Institute of Technology, 3-7-5 Toyosu, Koto-ku, Tokyo 135-8548, Japan.

T. Hauet is with the Institute Jean Lamour, Université de Lorraine, Vandœuvre-les-Nancy, France.

B. Douine and K. Berger are with GREEN, Université de Lorraine, Vandœuvre-les-Nancy, France.

II. Experimental Procedure

Several samples were fabricated using a solid state reaction in pure Ar atmosphere from 750 to 950 °C in order to determine the optimum processing parameters to obtain the highest critical current density, j_c, as well as large trapped field values. The X-ray analysis of these samples is presented elsewhere [11]. The magnetic characterization measurements were performed using SQUID magnetometry (Quantum Design MPMS) and the magneto-resistance charac-teristics were recorded using an Oxford Instruments 8 T Teslatron system. The critical current densities were calculated from the magnetization loops using the extended Bean model for rectangular samples. The trapped magnetic field was studied by magnetizing the bulk sample in a 10 T superconducting magnet over a wide temperature range between 20 K and 40 K. The transverse Hall sensor, which was directly glued at the center of the top and bottom surfaces of the bulk, has then only 0.5 mm distance between the probe and the surface of the sample. For SQUID measurements, small samples (2 × 2 × 1.5 mm^3) were cut from the big pellets.

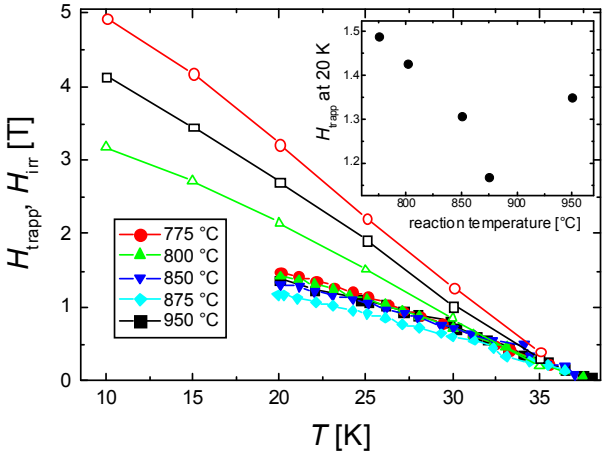

Fig. 1. The irreversibility lines (open symbols) and the measured trapped fields (full symbols) for several selected samples. The inset illustrates the recorded trapped fields at 20 K as a function of the reaction temperature.

For the resistance measurements, small bars (10 × 1 × 1 mm^3) were prepared, and the contacts were fixed with silver paint.

The AFM topography images were recorded using a Veeco/DI Nanoscope IV AFM employing micromachined Si-cantilevers.

III. Results and Discussion

As shown in Ref. [11], the samples prepared at temperatures lower than 775 °C are not pure MgB_2 phase, and the respective j_c is lower. The irreversibility fields, H_{irr}, are determined from the $M(H)$-loops using a criterion of 100 Acm^{-2}. Figure 1 indicates that the sample prepared at 775 °C exhibits the highest $H_{irr}(T)$ line, and also the highest trapped fields (measured only down to 20 K). $H_{irr}(T)$ and the trapped fields are then found to decrease when increasing the reaction temperature. However, the data of the sample processed at 950 °C show again an increase of $H_{irr}(T)$ and the trapped field (see the inset to Fig. 1). From the $M(H)$-loops recorded, we find that the sample processed at 775 °C showed the highest critical current density, j_c, of 176 $kAcm^{-2}$ and 55 $kAcm^{-2}$ at 20 K in self-field and the trapped field of 1 T, respectively. The critical current density values are increasing further to 250 kA cm^{-2} and 150 $kAcm^{-2}$ on decreasing the temperature further down to 10 K [10]. In order to understand this behavior, a more detailed investigation of the magnetic properties is required.

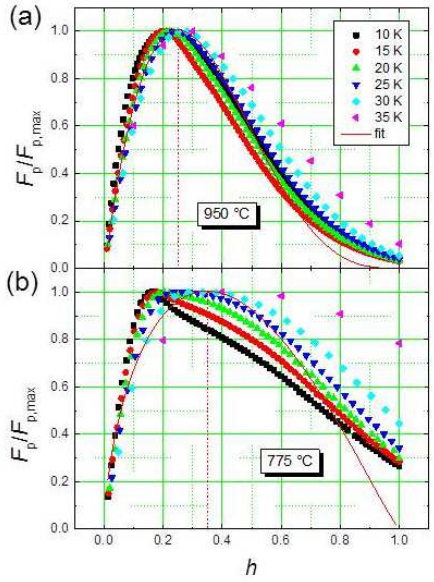

Fig. 2. Pinning force scaling for the sample prepared at 950 °C (a) and 775 °C (b). The shown fits are fits to *all* data. The dashed lines indicate the peak positions determined. The strong non-scaling of (b) is clearly visible.

The obtained magnetization data were evaluated further and transferred into a pinning force analysis, where the pinning force $F_p = j_c \times B$ is plotted versus a scaling field $h = H_a/H_{irr}$, with H_a denoting the applied magnetic field. [Figs. 2 (a,b)]. The resulting curves should scale according to $f(h) \sim h^p(1\text{-}h)^q$ as introduced by Dew-Hughes (DH) [12]. This analysis revealed for the sample prepared at 950 °C a well developed scaling of the normalized pinning force data at low and intermediate temperatures with the scaling parameters p = 0.65, q = 1.35 and a peak located at h_0 = 0.35 (data obtained from fit to all data, indicated by a red line). This would indicate pinning at normal conducting precipitates according to DH [12]. Similar values were obtained in the literature for small, pure MgB_2 samples, see e.g., the review of Ref. [13]. For a dominating flux pinning at the grain boundaries, $h_0 \sim$ 0.22 would be expected, which is not the case here.

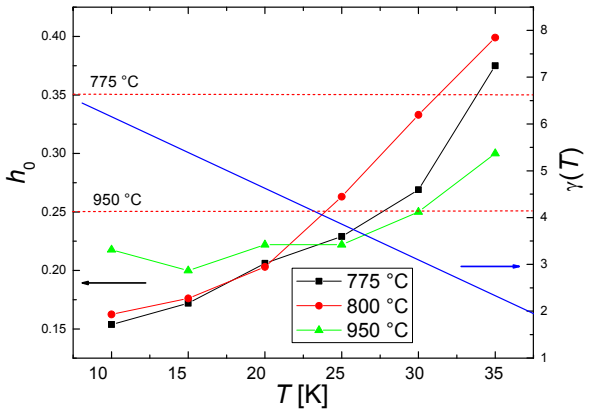

Fig. 3. The peak positions, h_0, of the $F_p(B)$-curves as a function of temperature. The values for h_0 as determined by the fits are indicated as dashed lines. Additionally, the temperature dependence of the anisotropy, γ(T), is shown according to Ref. [14].

In contrast to this behavior, the samples prepared at 775 and 800 °C reveal a clear non-scaling. As indicated in Fig. 2 (b), the resulting fit to all data cannot describe the situation. At higher T, the peak position shifts to h_0 = 0.4, and at low T, a peak position $h_0 < 0.2$ is reached. Peak positions $h_0 < 0.2$ cannot be explained by the common scaling model, except that the anisotropy γ or the percolation, p_c play a dominating role. This effect was discussed previously in Ref. [15], where j_c was calculated using the parameters γ = 4 and p_c = 0.25. This produces a shift of h_0 from 0.33 (isotropic case, point pinning) to about 0.18. This further implies that in order to deduce the acting pinning mechanism from the peak position of the pinning force scaling of MgB_2 samples, the anisotropy and percolation should be known. In Fig. 3, the resulting peak positions h_0 are shown as a function of temperature. Only the data of the sample prepared at 950 °C exhibits a plateau which is a prerequisite for the scaling, whereas the data of the other samples are continuously increasing with increasing temperature. Here, one should note the results of the DH fitting to all data as indicated by the dashed lines, being slightly larger than the individual peak positions. Additionally, the temperature dependence of the anisotropy parameter, γ(T), is plotted here. The anisotropy is changing with temperature according to $\gamma(T) = \gamma^* + k(1\text{-}T/T_c)$, where γ^* = 1.87 is the effective mass anisotropy and k = 6 [14]. As a result, γ(T) changes from 6 to 2 on increasing T, yielding h_0 = 0.158 to 0.33. In contrast to this, p_c is only slightly varying between 0.2 and 0.3 [15]. The large variation of h_0 obtained for the samples prepared at 775 and 800°C implies that the grain boundary character (connectivity) must change when processing the samples at higher reaction temperatures [16].

In Ref. [15], a different scaling procedure was suggested

where a field H_n is employed instead of H_{irr}. H_n is defined as the field where the pinning force F_p drops to 50% of its value above the peak position, i.e., all curves should pass the point (0.5,1) in the scaling diagram. The advantage of approach is that an area just below $h_n = 1$ exists which is not so sensitive to the effective values of γ and p_c. Figure 4 presents the results of this modified scaling procedure. In (a), a well developed scaling is obtained. The scaling reveals a peak at $h_n = 0.48$ (a) and 0.25-0.43 (b). For (a), this indicates dominating pinning at small precipitates, while in (b) the pinning is changing from grain boundary pinning to pinning at small precipitates. The data of Fig. 3 indicate that grain boundary pinning is significant only at low temperatures, whereas at higher temperatures, flux pinning at normal conducting precipitates plays the dominating role. As this conclusion also holds after applying the modified scaling procedure (see Fig. 4), this finding is an important one for the further development of MgB_2 bulk magnets.

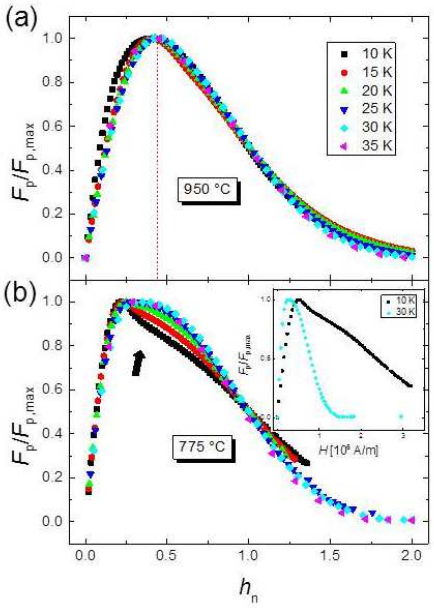

Fig. 4. Modified scaling procedure according to Ref. [15] using a scaling field, H_n, for the sample prepared at 950 °C (a) and at 775 °C (b). The arrow in (b) indicates the shape change at low temperatures, which is also visible in the $F_p(B)$ diagram (inset).

In Fig. 4 (b), the temperature dependence of the peak position is still visible. This further implies that p_c is changing with increasing reaction temperature, together with the grain size. Furthermore, the arrow points to a shape change of the curves at low T, which is also seen in the inset with the original $F_p(B)$ curves; the origin of which is discussed to be a competition of inter- and intragrain contributions to the pinning [17]. The change of the grain boundary character depending on the reaction temperature is also manifested in the resistance measurements (measured during field-cooled warming) as presented in Fig. 5. The magnetoresistance data reveal a much sharper superconducting transition for the sample prepared at 775 °C, whereas the transitions broaden up much more on increasing the magnetic field for the sample prepared at 950 °C. This also reflects the non-scaling of the pinning forces, as the $R(T,B)$ curves correspond to the $M(T,B)$ behavior as discussed in Refs. [18,19].

Microstructural observations obtained from scanning electron microscopy (SEM) and atomic force microscopy (AFM) indicated that the grain size is the crucial parameter to improve the critical currents as well as the trapped field values. This confirms the results of previous works [20-22]. Figure 6 presents typical AFM topography images of the samples recorded in the tapping mode. The images clearly reveal the polycrystalline nature of the sample. Individual MgB_2 grains show a specific crystallite shape and the dimensions of the grains are up to 400 nm. Obviously, the grain size and grain arrangement of (a) represents an optimal configuration, thus leading to the high trapped field values. The increase of the trapped fields for the sample prepared at 950 °C is attributed to the formation of nano-sized MgB_4 particles at the higher reaction temperature, which can provide additional, strong flux pinning by δT_c-pinning [23], but the worse character of the grain boundaries does not allow to reach the trapped field values of the sample prepared at 775 °C.

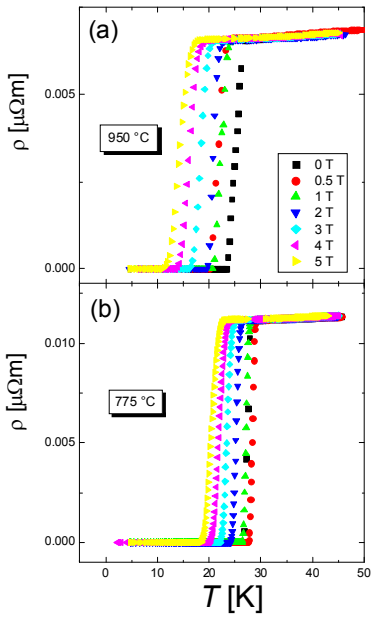

Fig. 5. Specific resistance as function of temperature for various applied fields for the sample prepared at 775 °C (a) and at 950 °C (b).

Another important aspect for the development of bulk, MgB_2-based supermagnets is the energizing procedure applied. MgB_2 suffers – in contrast to the bulk RE-123 samples – from flux jumps and the specific flux penetration in form of dendrites or avalanches, especially at low temperatures [24,25]. The microstructures shown in Fig. 6 directly confirm that the sample surface is inhomogeneous, formed of stacks of elongated grains with a length of up to 400 nm, and thus, a complicated percolative current flow takes place. The magnetization loops measured at 5 and 10 K with a sweep rate of 10 mT/s indicated the presence of flux

jumps. Therefore, for energizing MgB_2 supermagnets, it will be an essential task to develop a suited procedure, which may also include countermeasures like the application of a conductive thin-film cover onto the samples. A first attempt of such a procedure can be found already in Refs. [25,26], which indeed helps to reduce the number of flux jumps occurring in MgB_2 thin film samples. Tests are on the way also on bulk MgB_2 samples.

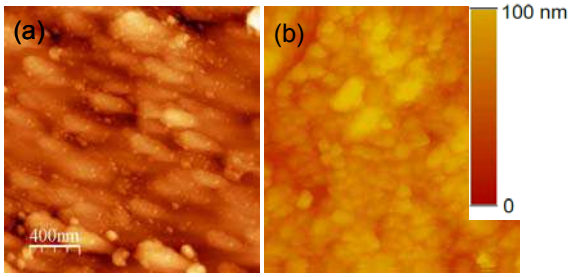

Fig. 6. AFM topography images (tapping mode) of the MgB_2 sample prepared at 775 °C (a) and of the sample prepared at 850 °C (b).

IV. Conclusion

To summarize, MgB_2 samples of 20 mm in diameter and 7 mm thickness, prepared with optimized processing temperature, exhibited a trapped field of ~1.5 T at 20 K. The characterization of small samples showed a change of flux pinning mechanisms as seen in the pinning force scaling. The current flow in the samples depends strongly on the grain boundary character, which gets worse on increasing the sintering temperature as revealed by the magnetoresistance measurements. 775 °C was found to be the optimum temperature to reach high trapped fields, while the sample prepared at 950 °C exhibits additional flux pinning provided by MgB_4 particles, however, due to the degraded grain boundaries, the trapped field achieved is not as high as of the sample prepared at 775 °C.

Acknowledgement

The collaboration Saarbücken-Nancy is supported by the INTERREG IVa project GRMN, which is gratefully acknowledged.

References

[1] K. Vinod, R. G. Abhilash Kumar and U. Syamaprasad, “Prospects for MgB_2 superconductors for magnet application”, *Supercond. Sci. Technol.*, vol. 20, pp. R1-R13, 2007.

[2] M. Tomsic, M. Rindfleisch, J. Yue, K. McFadden, J. Phillips, M.D. Sumption, M. Bhatia, S. Bohnenstiehl, E.W. Collings, “Overview of MgB_2 Superconductor Applications”, *Int. J. Appl. Ceram. Technol.*, vol. 4, pp. 250–259, July 2007.

[3] P. Mikheeko, E. Martinez, A. Bevan, J. S. Abell, and J. MacManus-Driscoll, “Grain boundaries and pinning in bulk MgB_2”, *Supercond. Sci. Technol.*, vol. 20, pp. S264-S270, 2007.

[4] E. Martinez, M. Martinez-Lopez, A. Millan, P. Mikheenko, A. Bevan and J. S. Abell, “Temperature and magnetic field dependence of the n-values of MgB_2 superconductors”, *IEEE Trans. Appl. Supercond.*, vol. 17, pp. 2738-2741, Jun. 2007.

[5] E. Martinez, P. Mikheenko, M. Martinez-Lopez, A. Millan, A. Bevan and J. S. Abell, “Flux pinning force in bulk MgB_2 with variable grain size”, *Phys. Rev. B*, vol. 75, p. 134515, 2007.

[6] S. X. Dou, S. Soltanian, J. Horvat, X. L. Wang, S. H. Zhou, M. Ionescu, H. K. Liu, P. Munroe and M. Tomsic, “Enhancement of the critical current density and flux pinning of MgB_2 superconductor by nanoparticle doping”, *Appl. Phys. Lett.*, vol. 81, pp. 3419-3421, 2002.

[7] A. Yamamoto, J. Shimoyama, S. Ueda, Y. Katsura, S. Horii and K. Kishio, “Improved critical current properties observed in MgB_2 bulks synthesized by low-temperature solid-state reaction”, *Supercond. Sci. Technol.*, vol. 18, pp.116-121, 2005.

[8] G. Giunchi, G. Ripamonti, T. Cavallin and E. Bassani, “The reactive liquid Mg infiltration process to produce large superconducting bulk MgB_2 manufacts”, *Cryogenics,* vol. 46, pp. 237-242, 2006.

[9] J.H. Durrell, C.E.J. Dancer, A. Dennis, Y. Shi, Z. Xu, A.M. Campbell, N. Hari Babu, R.I. Todd, C.R.M. Grovenor and D.A. Cardwell, “A trapped field of >3 T in bulk MgB_2 fabricated by uniaxial hot pressing”, *Supercond. Sci. Technol.*, vol. 25, p. 112002, 2012.

[10] T. Naito, T. Sasaki, and H. Fujishiro, “Trapped magnetic field and vortex pinning properties of MgB_2 superconducting bulk fabricated by a capsule method”, *Supercond. Sci. Technol.*, vol. 25, p. 095012 (2012).

[11] M. Muralidhar, K. Inoue, M.R. Koblischka, M. Tomita, and M. Murakami, "Optimization of processing conditions towards high trapped fields in MgB_2 bulks", submitted.

[12] D. Dew-Hughes, “Flux pinning mechanisms in type II superconductors”, *Philos. Mag.*, vol. 30, pp. 293-305, 1974.

[13] V. Sandu, “Pinning force scaling and its limitation in intermediate and high-temperature superconductors”, *Mod. Phys. Lett. B*, vol. 26, p 1230007, 2012.

[14] Z.X. Shi, M. Tokunaga, T. Tamegai, Y. Takano, K. Togano, H. Kito, and H. Ihara, “Out-of-plane and in-plane anisotropy of upper critical field in MgB_2”, *Phys. Rev. B*, vol. 68, p. 104513 (2003).

[15] M. Eisterer, “Calculation of the volume pinning force in MgB_2 superconductors”, *Phys. Rev. B*, vol. 77, p. 144524, 2008.

[16] M. Eisterer, “Magnetic properties and critical currents of MgB_2”, Supercond. Sci. Technol., vol. 20, pp. R47-R74, 2007.

[17] S.G. Jung, W. K. Seong and W. N. Kang, “Flux pinning mechanism in single-crystalline MgB_2 thin films”, *J. Phys. Soc. Jpn.*, vol. 82, p. 114712, 2013.

[18] M.R. Koblischka, M. Muralidhar, T. Higuchi, K. Waki, N. Chikumoto and M. Murakami, “Superconducting transitions of Nd-based 123 superconductors in fields up to 7 T”, *Supercond. Sci. Technol.*, vol. 12, pp. 288-292, 1992.

[19] A.K. Pradhan, M. Muralidhar, M.R. Koblischka, M. Murakami, K. Nakao and N. Koshizuka, “Evidence of strong flux pinning in melt-processed ternary (Nd-Eu-Gd)$Ba_2Cu_3O_y$ superconductors”, *Appl. Phys. Lett.*, vol. 75, pp.253-255, July 1999.

[20] M. Muralidhar, A. Ishihara, K. Suzuki, Y. Fukumoto, Y. Yamamoto and M. Tomita, “Optimization of the fabrication process for high trapped field MgB_2 bulks”, *Physica C*, vol. 494, pp. 85-88, 2013.

[21] M. Muralidhar, Y. Fukumoto, A. Ishihara, K. Suzuki, M. Tomita, M.R. Koblischka, A. Yamamoto and K. Kishio, “Recent developments in melt processed Gd-123 and MgB_2 materials at RTRI”, *Physica C*, vol. 496, pp. 5-10, 2014.

[22] G. Fuchs, W. Häßler, K. Nenkov, J. Scheiter, O. Perner, A. Handstein, T. Kanai, L. Schultz and B. Holzapfel, “High trapped fields in bulk MgB_2 prepared by hot-pressing of ball-milled precursor powder”, *Supercond. Sci. Technol.*, vol. 26, p. 122002, 2012.

[23] Q. Cai, Y. Liu, Z. Ma, H. Li and L. Yu, „Variation of pinning mechanism and enhancement of critical current density in MgB_2 bulk containing self-generated coherent MgB_4 impurity“, *Appl. Phys. Lett.*, vol. 103, p. 132601, 2013.

[24] D. V. Denisov, D. V. Shantsev, Y. M. Galperin, E.-M. Choi, H.-S. Lee, S.-I. Lee, A. V. Bobyl, P. E. Goa, A. A. F. Olsen, and T. H. Johansen, “Onset of dendritic flux avalanches in superconducting films”, *Phys. Rev. B*, vol. 73, p. 014512, 2006.

[25] F. Colauto, E. M. Choi, J.Y. Lee, S. I. Lee, V.V. Yurchenko, T. H. Johansen and W. A. Ortiz, “Mapping flux avalanches in MgB_2 films – equivalence between magneto-optical imaging and magnetic measurements”, *Supercond. Sci. Technol.*, vol. 20, pp. L48-L50, 2007.

[26] C. Stahl, S. Treiber, G. Schütz and J. Albrecht, “The avalance process in gold covered MgB_2 films”, *Supercond. Sci. Technol.*, vol. 26, p. 015007, 2013.